Acta Pharmacologica Sinica

www.nature.com/aps

ARTICLE

SAF-248, a novel PI3Kδ-selective inhibitor, potently suppresses the growth of diffuse large B-cell lymphoma

Xi Zhang[1], Yu-ting Duan[1,2], Yi Wang[1], Xing-dong Zhao[3], Yi-ming Sun[1], Dong-ze Lin[1], Yi Chen[1,2], Yu-xiang Wang[1], Zu-wen Zhou[3], Yan-xin Liu[3], Li-hua Jiang[3], Mei-yu Geng[2,4], Jian Ding[2,4] and Ling-hua Meng[1,2]

PI3Kδ is expressed predominately in leukocytes and overexpressed in B-cell-related malignances. PI3Kδ has been validated as a promising target for cancer therapy, and specific PI3Kδ inhibitors were approved for clinical practice. However, the substantial toxicity and relatively low efficacy as a monotherapy in diffuse large B-cell lymphoma (DLBCL) limit their clinical use. In this study, we described a novel PI3Kδ inhibitor SAF-248, which exhibited high selectivity for PI3Kδ (IC_{50} = 30.6 nM) over other PI3K isoforms at both molecular and cellular levels, while sparing most of the other human protein kinases in the kinome profiling. SAF-248 exhibited superior antiproliferative activity against 27 human lymphoma and leukemia cell lines compared with the approved PI3Kδ inhibitor idelalisib. In particular, SAF-248 potently inhibited the proliferation of a panel of seven DLBCL cell lines (with GI_{50} values < 1 μM in 5 DLBCL cell lines). We demonstrated that SAF-248 concentration-dependently blocked PI3K signaling followed by inducing G_1 phase arrest and apoptosis in DLBCL KARPAS-422, Pfeiffer and TMD8 cells. Its activity against the DLBCL cells was negatively correlated to the protein level of PI3Kα. Oral administration of SAF-248 dose-dependently inhibited the growth of xenografts derived from Pfeiffer and TMD8 cells. Activation of mTORC1, MYC and JAK/STAT signaling was observed upon prolonged treatment and co-targeting these pathways would potentiate the activity of SAF-248. Taken together, SAF-248 is a promising selective PI3Kδ inhibitor for the treatment of DLBCL and rational drug combination would further improve its efficacy.

Keywords: PI3Kδ; PI3K/AKT/mTOR; diffuse large B-cell lymphoma; resistance; combination therapy

Acta Pharmacologica Sinica (2022) 43:209–219; https://doi.org/10.1038/s41401-021-00644-1

INTRODUCTION

Diffuse large B-cell lymphoma (DLBCL), the most common subtype of B-cell non-Hodgkin lymphoma, is an aggressive and heterogeneous disease with a high risk of treatment failure [1]. Although approximately 60% of patients with DLBCL can be cured by the standard-of-care therapy with rituximab plus cyclophosphamide, doxorubicin, vincristine, and prednisone (R-CHOP), 30%–40% of patients exhibit resistance to this treatment or relapse after a complete response [2, 3]. Currently, effective therapeutic options available for refractory or relapsed patients are extremely limited, indicating an unmet therapeutic need. As a result, many efforts have been made toward developing novel and more effective therapeutic approaches. DLBCL can be divided into two major molecular subtypes with distinct genomic profiles, termed germinal center B-cell-like (GCB) and activated B-cell-like (ABC). The B-cell receptor (BCR) and the downstream phosphatidylinositol 3-kinase (PI3K) are frequently hyperactivated in both GCB- and ABC-DLBCL [4] and have emerged as important therapeutic targets for DLBCL.

PI3K integrates multiple signals from growth factors and cytokines and further activates the AKT/mTOR pathway to play crucial roles in regulating cell proliferation, migration, and survival [5]. Mammalian PI3Ks are categorized into three groups (I, II, and III), and class I PI3Ks are further divided into class IA PI3Ks (PI3Kα, β, and δ) and the class IB PI3K (PI3Kγ) [6]. PI3Kδ is enriched in hematopoietic cells and activated by T- and B-cell antigen receptors [7, 8]. PI3Kδ is involved in BCR signaling and possesses an important function in the survival and differentiation of B cells. Selective targeting of PI3Kδ has been validated as a promising approach for cancer therapy. Idelalisib was the first PI3Kδ-selective inhibitor approved by the FDA for the treatment of chronic and relapsed chronic lymphocytic leukemia (CLL), follicular lymphoma (FL), and small lymphocytic lymphoma (SLL). Although idelalisib has demonstrated significant clinical efficacy, it causes serious toxicity, leading to its approval tagged with a black box warning. Idelalisib failed to achieve desirable responses in relapsed/refractory DLBCL patients, suggesting its lack of efficacy as a monotherapy against DLBCL [9]. Duvelisib, a second-generation PI3Kδ/γ dual inhibitor that displays enhanced efficacy against DLBCL [10], was recently approved for the treatment of FL, CLL, and SLL after two or more systemic therapies. Copanlisib, an approved pan-class I PI3K inhibitor, and fimepinostat, a dual inhibitor of histone deacetylase and PI3K, have shown potential in treating DLBCL [11, 12]. Although preliminary efficacy has been shown in DLBCL by targeting the PI3K pathway [13], unexpected side effects, especially those related to pan-PI3K inhibitors, have

[1]Division of Anti-tumor Pharmacology, Shanghai Institute of Materia Medica, Chinese Academy of Sciences, Shanghai 201203, China; [2]University of Chinese Academy of Sciences, Beijing 100049, China; [3]Fochon Pharmaceuticals, Ltd., Chongqing 404100, China and [4]Division of Anti-Tumor Pharmacology, State Key Laboratory of Drug Research, Shanghai Institute of Materia Medica, Chinese Academy of Sciences, Shanghai 201203, China
Correspondence: Mei-yu Geng (mygeng@simm.ac.cn) or Jian Ding (jding@simm.ac.cn) or Ling-hua Meng (lhmeng@simm.ac.cn)

Received: 22 December 2020 Accepted: 9 March 2021
Published online: 29 March 2021

limited the clinical applications of PI3K inhibitors [14]. Because of the critical role of PI3Kδ in DLBCL, there is a great need to discover novel PI3Kδ-selective inhibitors that exhibit improved potency. On the other hand, a number of patients do not respond to PI3Kδ inhibitors, and a fraction of patients develop resistance upon continuous treatment, which eventually leads to disease progression [15, 16]. Rational drug combination is a promising strategy to overcome drug resistance and enhance efficacy without significant toxicity. Currently, several clinical trials are underway to evaluate the combination of PI3Kδ inhibitors with other molecularly targeted agents for the treatment of DLBCL, e.g., the combination of idelalisib with the spleen tyrosine kinase (SYK) inhibitor entospletinib (NCT01796470) and fimepinostat with the B-cell lymphoma-2 inhibitor (Bcl-2) inhibitor venetoclax (NCT01742988). A better understanding of the mechanism of DLBCL resistance to PI3Kδ inhibitors will facilitate the development of new drug combination regimens.

In an effort to discover novel PI3Kδ-selective inhibitors, a series of pyridone ring derivatives were designed, synthesized and evaluated [17]. SAF-248 was identified as a novel PI3Kδ-selective inhibitor with a distinctive structure and potent antiproliferative activity against a wide spectrum of B-cell lymphomas and leukemia. Here, we describe the in vitro and in vivo potency of SAF-248 against DLBCL and reveal the synergistic inhibition of PI3Kδ with inhibitors targeting pathways critical for DLBCL, which may be useful for the further clinical development of PI3Kδ inhibitors in the treatment of DLBCL.

MATERIALS AND METHODS

Compounds

SAF-248 was provided by Fochon Pharmaceuticals, Ltd. (Chongqing, China). Idelalisib, alpelisib, bortezomib, doxorubicin, methotrexate, bleomycin sulfate, vincristine, vinblastine, mechlorethamine HCl, everolimus, ruxolitinib, pacritinib, fludarabine, entospletinib, and venetoclax were purchased from Selleck Chemicals (Houston, TX, USA). All compounds were dissolved at 10 mM in dimethyl sulfoxide (DMSO; Sigma-Aldrich, St. Louis, MO, USA) as stock solutions, and aliquots were stored at −20 °C. Compounds were diluted to the desired concentration before each experiment. For the in vivo studies, compounds were dissolved in normal saline containing 30% polyethylene glycol (PEG) 400 (*v/v*; Sangon Biotech, Shanghai, China), 0.5% Tween 80 (*v/v*, Sangon Biotech, Shanghai, China) and 5% propylene glycol (*v/v*, Sangon Biotech, Shanghai, China).

In vitro PI3K assay

The effect of the tested compounds on the PI3K activity was assessed using a PI3-Kinase HTRF™ Assay kit (Sigma-Aldrich, St. Louis, MO, USA) as described previously [18]. In brief, the EC_{80} concentration of each enzyme containing 10 μM PIP2 was mixed with each tested compound in assay buffer. The reaction was initiated by adding ATP and terminated by adding stop solution after 30-min of incubation at room temperature. The intensity of the light emission was measured with an EnVision Multilabel Reader (PerkinElmer, Inc., Waltham, MA, USA), and the IC_{50} values were calculated by fitting the data to a logistic curve using GraphPad Prism 7 software (GraphPad Software, Inc., San Diego, CA, USA). In vitro kinase profiling was performed by the Kinase Profiler Service following its guidelines (Eurofins Pharma Discovery Services UK Limited, Dundee, UK).

Cell lines and cell culture

Human lymphoma U2932, KARPAS-422, SU-DHL-4, RL, WSU-DLCL2, OCI-LY-19, DB, HT, L-428, and KARPAS-299 cells were obtained from the Leibniz Institute DSMZ-German Collection of Microorganisms and Cell Culture GmbH (DSMZ, Braunschweig, Germany). SU-DHL-6, Pfeiffer, KG-1, JEKO-1, Z-138, MM.1S, Jurkat, HH, Molt-4, HEL, NIH-3T3, PC-3, RAW264.7 and Ramos cells were obtained from the American Type Culture Collection (ATCC, Manassas, VA, USA). TMD8, OCI-LY-10 and MV-4-11 cells were obtained from the Cell Bank of the Chinese Academy of Sciences (Shanghai, China). MOLM-13, WIL-2-NS, and KMS-11 cells were obtained from the Japanese Collection of Research Bioresources Cell Bank (JCRB, Osaka, Japan). Eol-1 cells were obtained from the European Collection of Authenticated Cell Cultures (ECACC, Salisbury, UK). Cell lines were authenticated by analyzing short tandem repeats by Genesky Biotechnologies Inc. (Shanghai, China). All cells were maintained in the appropriate culture medium suggested by the suppliers.

Cell proliferation assay

Cell proliferation was measured by a Cell Counting Kit (CCK-8, Dojindo, Kumamoto, Japan) as described previously [19]. Briefly, cells seeded in 96-well plates were treated with diluted compounds in triplicate for 72 h. CCK-8 reagent was added to each well, and the optical density (*OD*) value was measured at 450 nm using a multiwell spectrophotometer (Molecular Devices, Sunnyvale, CA, USA). The inhibitory rate was calculated using the following formula: $(OD_{\text{control cells}} - OD_{\text{treated cells}} - OD_{\text{Day 0}})/(OD_{\text{control cells}} - OD_{\text{Day 0}}) \times 100\%$, where $OD_{\text{Day 0}}$ indicates the *OD* of the control cells immediately before treatment. GI_{50} values were calculated by using GraphPad Prism 7 software.

Western blot

Cell lysates were harvested and subjected to standard Western blot analysis using antibodies against phospho-AKT (Ser473), phospho-AKT (Thr308), AKT, phospho-p70 S6 Kinase (p70S6K, Thr389), p70S6K, phospho-S6 Ribosomal Protein (S6, Ser235/236), phospho-S6 (Ser240/244), S6, phospho-4E-BP1 (Thr37/46), 4E-BP1, phospho-Erk1/2 (Thr202/Tyr204), Erk1/2, phospho-signal transducer and activator of transcription (STAT)3 (Tyr705), STAT3, phospho-STAT5 (Tyr694), STAT5, MYC, PI3Kα, PI3Kβ, PI3Kδ, PI3Kγ, cleaved caspase 3, caspase 3 (Cell Signaling Technology, Inc., Danvers, MA, USA), and β-actin (Sigma-Aldrich, St. Louis, MO, USA).

Flow cytometry

Cell cycle distribution was assessed with a FACSCalibur™ Instrument (BD Biosciences, San Jose, CA, USA) as previously reported [20]. To detect apoptosis, cells were cultured in the presence of the tested compounds for 72 h. Apoptotic cells were measured by annexin V-fluorescein isothiocyanate and 7-aminoactinomycin D (7-AAD) (BD Biosciences, San Jose, CA, USA) staining, followed by flow cytometry analysis. Data were analyzed with FlowJo software (BD Biosciences, San Jose, CA, USA).

Animal experiments

All experiments were performed according to the institutional ethical guidelines on animal care and were approved by the Institute of Animal Care and Use Committee at Shanghai Institute of Materia Medica. Four-to-five-week-old female BALB/c athymic nude mice were obtained from the Shanghai Institute of Materia Medica (Shanghai, China). Human tumor xenografts derived from TMD8 or Pfeiffer cells were established. Tumor-bearing mice were orally administered vehicle, idelalisib or SAF-248 at the indicated dose twice daily. The body weights and tumor volumes of each group ($n = 6$) were measured and recorded twice per week. The tumor volume (*V*) was calculated by the formula: $V = 0.5 \times \text{length (mm)} \times \text{width}^2\ (\text{mm}^2)$. The relative tumor volume (RTV) was calculated at each measurement time point using the formula: RTV = tumor volume at the given time point/initial tumor volume. The treatment-to-control ratio (*T/C*) was calculated using the following formula: $T/C\ (\%) = (T_{RTV}/C_{RTV}) \times 100\%$, where T_{RTV} and C_{RTV} represent the RTV of the treatment and vehicle groups, respectively.

Pharmacokinetic/pharmacodynamic studies were performed as described previously [21]. Mice bearing TMD8 tumors were randomly divided into three groups (three mice/group) and were given vehicle or SAF-248 at 100 mg/kg. Tumor tissues and blood were collected 2 h or 4 h after administration of SAF-248, respectively. Concentrations of SAF-248 in plasma and tissue were measured by HPLC/tandem mass spectrometry. Tumor tissues were homogenized and processed for Western blot analysis.

RNA sequencing

Samples from xenograft tumors were collected, and RNA sequencing was performed by WuXi AppTec using Illumina-HiSeq (Shanghai, China). Differentially expressed genes were identified with a fold change cutoff of 1.5. Pathway enrichment analysis was assessed using Gene Set Enrichment Analysis (GSEA, http://software.broadinstitute.org/gsea/index.jsp).

Combination assay

Cells were treated with a single agent alone or in combination with another agent, and the inhibitory rate of cell proliferation was assessed by CCK-8 assay. The combination index (CI) was analyzed by CalcuSyn software as described previously (Biosoft, Cambridge, UK) [22].

Statistical analysis

Data presented are from at least two independent experiments. Statistical analysis was performed using Student's *t* test. Differences were considered statistically significant when the *P* value was less than 0.05.

RESULTS

SAF-248 is a potent and selective PI3Kδ inhibitor

To discover novel and selective PI3Kδ inhibitors, we designed and synthesized a series of pyridone ring derivatives based on previously reported PI3Kδ inhibitors [23]. High-throughput screening was performed to evaluate the activity of these derivatives against the kinase activity of PI3Kδ. SAF-248 was identified as a potent PI3Kδ-selective inhibitor. As shown in Fig. 1a, SAF-248 significantly inhibited the enzymatic activity of PI3Kδ with an IC_{50} of 30.6 nM, which is much lower than the IC_{50} values determined against other class I PI3K enzymes. Idelalisib, a clinically approved PI3Kδ inhibitor, displayed a similar profile against the four class I PI3K isoforms. To further characterize the selectivity of SAF-248, we tested its activity against a panel of 318 human kinases. Of all the tested protein kinases, none of them were inhibited by greater than 50% in the presence of 10 μM SAF-248. However, SAF-248 exhibited significant inhibitory activity against a few lipid kinases, including isoforms and mutated PI3Ks, at this same concentration (Fig. 1b). To further confirm the selectivity of SAF-248 among class I PI3Ks, we investigated the activity of SAF-248 against PI3K at the cellular level by examining the phosphorylation of AKT at S473, a surrogate marker for cellular PI3K activity [24]. The individual isoform of PI3K is known to be activated by different extracellular stimuli in particular cell contexts [25, 26]. Platelet-derived growth factor BB (PDGF-BB) triggers the PI3K-AKT pathway via PI3Kα in NIH-3T3 murine fibroblast cells, while lysophosphatidic acid (LPA) and C5a stimulate G-protein coupled receptor signals mediated by PI3Kβ or PI3Kγ in PC-3 human prostate cancer cells or RAW264.7 mouse macrophage cells, respectively. Stimulation of Ramos human Burkitt's lymphoma cells with anti-IgM leads to the activation of PI3Kδ. As shown in Fig. 1c, phosphorylation of AKT at S473 was induced in the presence of each indicated stimulus in the cells tested, indicating the activation of each stimulus-related PI3K isoform. SAF-248 at 1 nM significantly blocked PI3Kδ-mediated AKT phosphorylation in Ramos cells stimulated by anti-IgM, while a much higher concentration of SAF-248 was required to inhibit the phosphorylation of AKT induced by the other three class I PI3K isoforms. A similar pattern was observed in the presence of idelalisib. Thus, these results indicate that SAF-248 is a potent and selective PI3Kδ inhibitor.

SAF-248 exhibits significant antiproliferative activity against DLBCL cells

PI3Kδ plays a critical role in cell growth and proliferation in hematological malignancies. We assessed the antiproliferative activity of SAF-248 against 27 cancer cell lines derived from different types of hematological malignancies. As shown in Fig. 2a, SAF-248 displayed potent antiproliferative activity with GI_{50} values lower than 1 μM in 29.6% (8/27) of the tested cell lines. However, GI_{50} values are highly variable, ranging from 0.7 nM in TMD8 cells to over 10 μM in HEL and Eol-1 cells. SAF-248 exhibited a similar profile but enhanced activity compared with idelalisib, as the GI_{50} values of SAF-248 were 2–3-fold lower than those of idelalisib, indicating that SAF-248 and idelalisib shared similar targets but SAF-248 exhibited superior antiproliferative activity.

SAF-248 markedly inhibited the proliferation of the tested ABC- and GCB-DLBCL cells, with GI_{50} values below 1 μM in five DLBCL cell lines (Fig. 2b), which was consistent with a previous report that PI3Kδ was hyperactivated in DLBCL [27, 28]. To explore the association of the level of PI3K and the activity of SAF-248 in DLBCL cells, we detected the protein levels of four isoforms of class I PI3Ks and phosphorylated AKT in three ABC-DLBCL cell lines and four GCB-DLBCL cell lines (Fig. 2c). Although cells with higher expression of PI3Kδ tended to be more sensitive to SAF-248, there was no significant correlation between the cellular GI_{50} values and PI3Kδ protein levels (Fig. 2e). Similarly, the level of phosphorylated AKT failed to correlate with the activity of SAF-248. Unexpectedly, cell lines with low PI3Kα expression were significantly more sensitive to SAF-248 than those with high-expression levels (Fig. 2d), as evidenced by a correlation coefficient of 0.77 between the PI3Kα level and GI_{50} values of SAF-248 in the seven tested DLBCL cell lines. These findings indicate that PI3Kα may compensate for PI3Kδ inhibition, which may lead to resistance to PI3Kδ inhibitors in DLBCL cells. To investigate whether inhibition of PI3Kα could restore sensitivity to SAF-248 in insensitive cell lines, the combinatorial effect of SAF-248 and alpelisib, the first FDA-approved PI3Kα inhibitor, against the proliferation of OCI-LY19 cells was assessed. As shown in Fig. 2f, the inhibitory rate of the combined treatment (both at 300 nM) was significantly higher than that in the presence of SAF-248 alone, indicating that simultaneous inhibition of PI3Kδ and PI3Kα could display enhanced antiproliferative activity.

SAF-248 blocks the downstream signaling mediated by PI3K in DLBCL cells

As SAF-248 displayed potent antiproliferative activity in a panel of DLBCL cell lines, we next determined the effects of SAF-248 on PI3K signaling in GCB-DLBCL KARPAS-422 and Pfeiffer cells, as well as ABC-DLBCL TMD8 cells, where PI3K/AKT signaling is constitutively activated due to PTEN loss or BCR activation [28–30]. As shown in Fig. 3a, SAF-248 inhibited the phosphorylation of AKT at S473 and T308 in a concentration-dependent manner in all DLBCL cells tested. Treatment with SAF-248 at 10 μM for 1 h resulted in decreased AKT phosphorylation by 20%–50%, while a much lower concentration of SAF-248 was required to inhibit the phosphorylation of p70S6K1, 4E-BP1, or S6 in KARPAS-422 cells (Fig. 3b), suggesting an amplified cascade in signal blockade. Interestingly, a similar phenomenon was not observed in other GCB-DLBCL Pfeiffer cells, where phosphorylation of AKT and its downstream factors displayed similar levels of inhibition in the presence of the same concentration of SAF-248. As shown in Fig. 3b, phosphorylation of AKT at S473 decreased by 39.5% in Pfeiffer cells treated with 10 μM SAF-248, while phosphorylation of p70S6K1 at T389, 4E-BP1 at T37/46 and S6 at S240/244 decreased by 52.2%, 43.5%, and 57.0%, respectively. In contrast, SAF-248 potently inhibited

a

Compound	IC_{50} (nM)			
	PI3Kα	PI3Kβ	PI3Kδ	PI3Kγ
SAF-248	1052.2 ± 346.0	322.1 ± 77.8	30.6 ± 10.7	184.2 ± 11.0
Idelalisib	6108.5 ± 984.0	720.5 ± 42.4	13.5 ± 4.8	322.0 ± 17.1

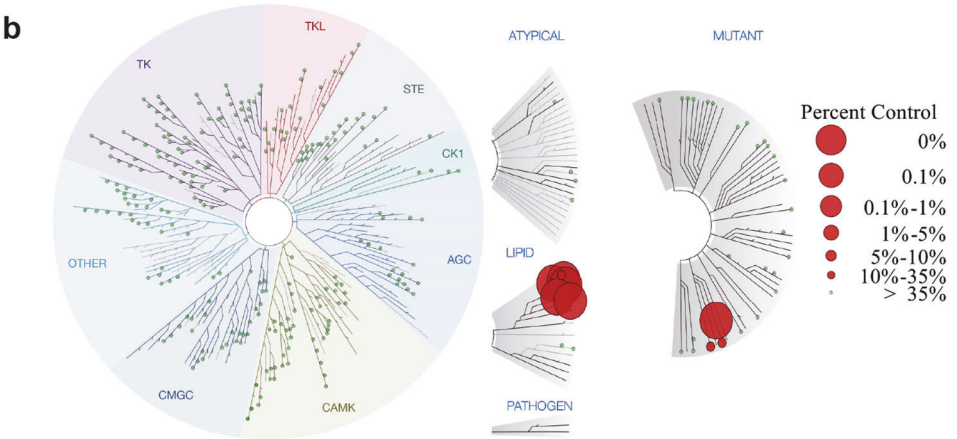

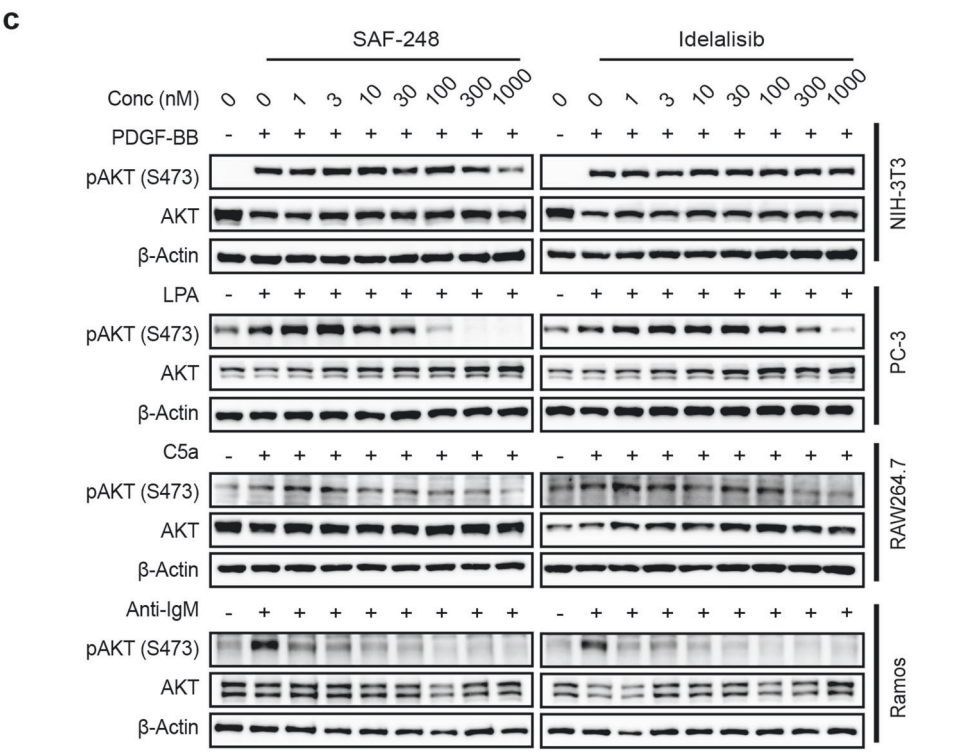

Fig. 1 SAF-248 is a potent and selective PI3Kδ inhibitor. a Inhibitory activities of SAF-248 and idelalisib on the kinase activity of human class I PI3K family members. The IC_{50} values shown are the mean ± SD from three independent experiments. **b** TreeSpot™ kinase profiling map of SAF-248 against over 300 human kinases. The dendrogram was generated utilizing the TREEspot Software Tool, DiscoveRx KinomeScan™. **c** SAF-248 preferentially inhibited PI3Kδ at the cellular level. NIH-3T3, PC-3, RAW264.7, and Ramos cells were starved in serum-free medium overnight and treated with SAF-248 for 30 min before stimulation with PDGF-BB (20 ng/mL), LPA (10 μM), C5a (200 ng/mL), and anti-IgM (3 μg/mL), respectively. Phosphorylation of AKT at Ser473 was detected. Representative images are presented.

the phosphorylation of AKT at 10 nM, but it was much less effective in inhibiting phosphorylation of 4E-BP1 at T37/46 in TMD8 cells, perhaps due to the existence of alternative regulator upstream mTOR in TMD8 cells. In addition, significantly reduced phosphorylation of AKT was observed in TMD8 cells treated with SAF-248 at concentrations as low as 1 nM, which is similar to the concentration required to block the biochemical activity of PI3Kδ, indicating a major role of PI3Kδ in constitutive PI3K signaling in TMD8 cells. Thus, SAF-248 potently inhibits constitutive PI3K signaling in DLBCL cells.

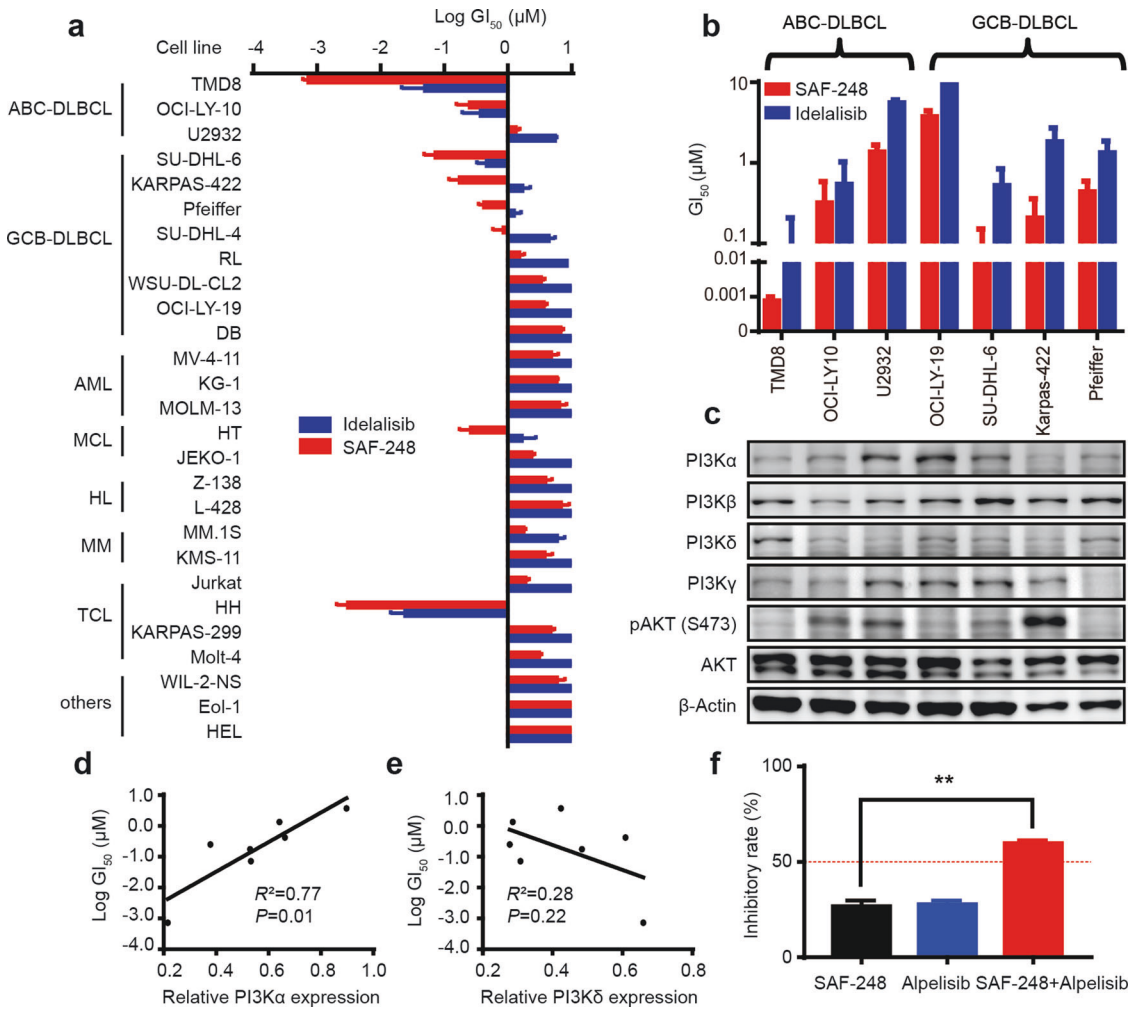

Fig. 2 SAF-248 exhibits significant antiproliferative activity against DLBCL cells. a The antiproliferative activity of SAF-248 and idelalisib against a panel of tumor cell lines derived from hematological malignancies was determined by the CCK-8 assay. The GI_{50} values were calculated and plotted. The GI_{50} was assigned as 10 μM when the inhibitory rate was less than 50% at 10 μM. The data shown represent the mean ± SD of three independent experiments. Abbreviations: AML, acute myeloid leukemia; HL, Hodgkin lymphoma; MM, multiple myeloma; TCL, T-cell lymphoma. **b** GI_{50} values of SAF-248 and idelalisib in the panel of DLBCL cell lines. Data presented are the mean ± SD of three independent experiments. **c** Expression of the indicated proteins in the tumor cell lines was detected by Western blot. Correlation analysis between the log GI_{50} values and relative protein expression of PI3Kα (**d**) and PI3Kδ (**e**). The correlation was analyzed by GraphPad Prism 7 software. **f** The combinatorial effect of SAF-248 and alpelisib against the proliferation of OCI-LY-19 cells. Cells were seeded in 96-well plates and incubated with the indicated compounds for 72 h. Cell proliferation was detected by CCK-8 assay. Statistical differences were analyzed with Student's *t* test. $^{**}P < 0.01$. The data shown represent the mean ± SD from two independent experiments.

We also observed that treatment of TMD8 cells with SAF-248 resulted in a time-dependent reduction in the phosphorylation of AKT, p70S6K, and S6 (Fig. 3c). Both AKT and p70S6K phosphorylation were readily inhibited after treatment for 15 min to 6 h, whereas phosphorylation of S6 at S240/244 and S235/236 started to decrease after at least 1 h of treatment (Fig. 3c). To test whether the effects of SAF-248 on PI3K signaling are reversible, TMD8 cells were incubated in drug-free medium following treatment with 10 nM SAF-248 for 1 h. As shown in Fig. 3c, restoration of the phosphorylation of AKT and S6 could be observed at 15 min to 1 h after SAF-248 removal, indicating that the action of SAF-248 on PI3K is rapidly reversible. This finding indicates that continuous inhibition of PI3K may be required to maintain the effectiveness of SAF-248.

SAF-248 induces cell cycle arrest and apoptosis in DLBCL cells

Given that PI3Kδ plays an important role in B-cell survival and regulates the G_1-S phase transition in the cell cycle, we investigated the effects of SAF-248 on cell proliferation and the cell cycle in DLBCL cells. We found that SAF-248 potently inhibits the proliferation of KARPAS-422, Pfeiffer and TMD8 cells with GI_{50} values of 206.0 nM, 436.4 nM, and 0.7 nM, respectively (Fig. 4a–c). This result implied that SAF-248 showed similar antiproliferative activity against GCB-DLBCL KARPAS-422 and Pfeiffer cells while exerting potent antiproliferative activity against ABC-DLBCL TMD8 cells, which may reflect the PI3Kδ-dependent cell proliferation in TMD8 cells. To further investigate the mechanism of SAF-248-induced antiproliferative activity in DLBCL cells, we evaluated the effects of SAF-248 on the cell cycle distribution. As shown in Fig. 4d, treatment with SAF-248 at various concentrations for 24 h increased the cell population in G_1 phase accompanied by a decreased cell population in S phase, indicating that the inhibition of PI3Kδ by SAF-248 led to the blockade of cell cycle progression. The cell population in G_1 phase increased in a dose-dependent manner in Pfeiffer cells, while increasing concentrations of SAF-248 in KARPAS-422 and TMD8 cells failed to further accumulate cells in G_1 phase (Fig. 4d). Prolonged cell cycle arrest may induce cell apoptosis. As shown in Fig. 4e, the number of annexin

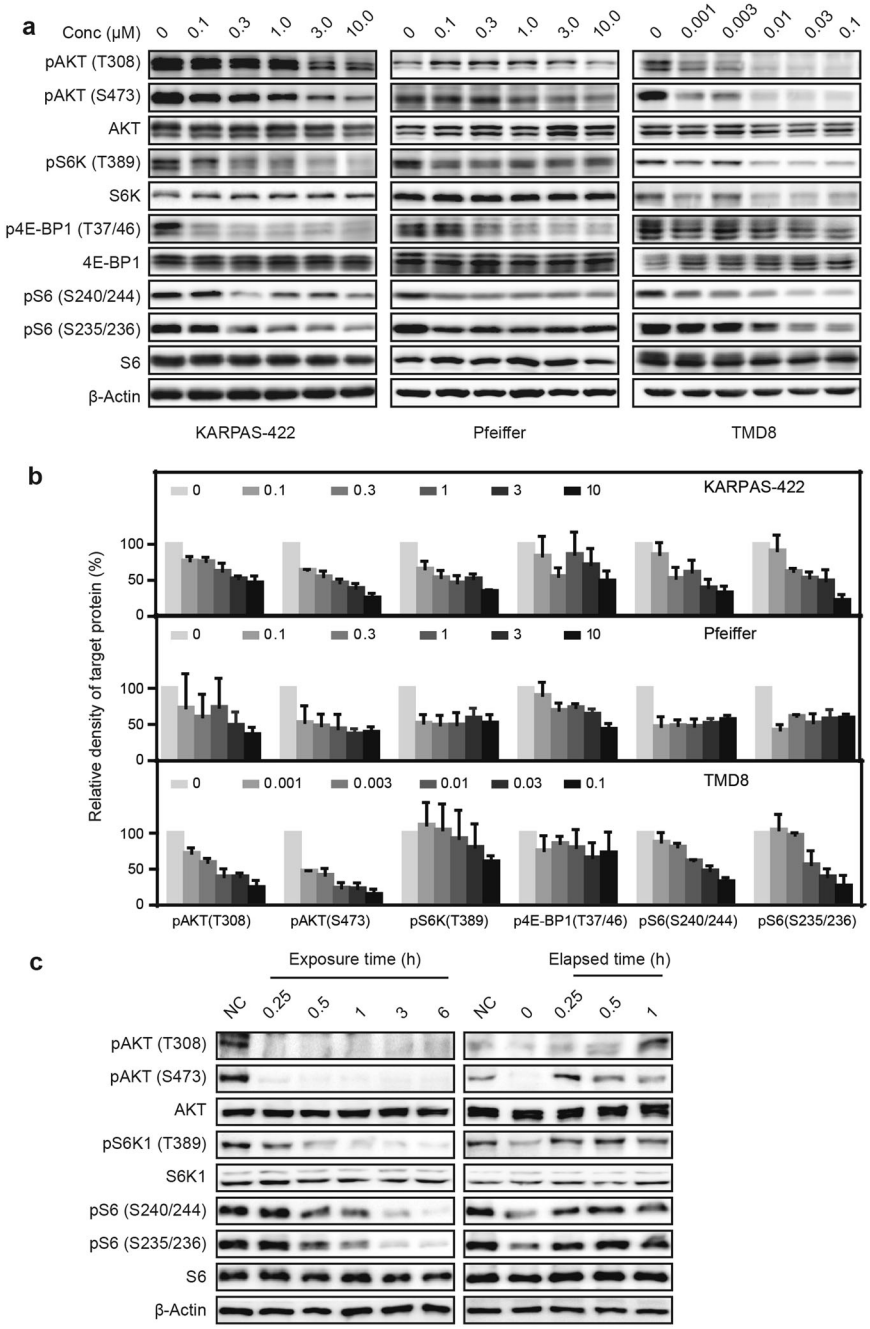

Fig. 3 SAF-248 blocks PI3K-mediated signaling. a SAF-248 concentration-dependently inhibited the phosphorylation of AKT and its downstream signals. KARPAS-422, Pfeiffer and TMD8 cells were treated with SAF-248 for 1 h at the indicated concentrations, and cell lysates were subjected to Western blot analysis with the indicated antibodies. **b** The level of phosphorylated protein was determined by normalization of the phosphorylated protein to the respective total protein. The intensity of the protein bands was quantified with ImageJ software. The data shown are the mean ± SD from at least two independent experiments. **c** SAF-248 time-dependently inhibited PI3K/AKT signaling. TMD8 cells were treated with 10 nM SAF-248 for the indicated times (left panel). TMD8 cells were incubated in fresh medium following treatment with 10 nM SAF-248 for 1 h (right panel). Cell lysates were collected at the indicated times and subjected to Western blot with the indicated antibodies.

V-positive cells increased significantly in DLBCL cells tested after treatment with SAF-248 for 72 h. An increase in the level of cleaved caspase 3 was observed (Fig. 4f), which confirmed apoptosis induction by SAF-248. SAF-248 was more potent in inducing apoptosis in TMD8 cells than in KARPAS-422 and Pfeiffer cells, which was consistent with its superior antiproliferative activity in TMD8 cells compared to the other two cell lines. These results suggest that inhibition of PI3Kδ by SAF-248 results in the blockade of cell cycle progression, and longer treatment induces cell apoptosis. Therefore, SAF-248 induces cell cycle arrest at G_1 phase and apoptosis in DLBCL cells.

SAF-248 suppresses the growth of Pfeiffer and TMD8 xenografts

Given the encouraging activity of SAF-248 in DLBCL cells, we next investigated the antitumor effects of SAF-248 in xenografts derived from DLBCL cells. Oral administration of SAF-248 twice a day for 21 days significantly inhibited the growth of Pfeiffer xenografts with *T/C* values of 46.7% and 43.5% at doses of 30 and

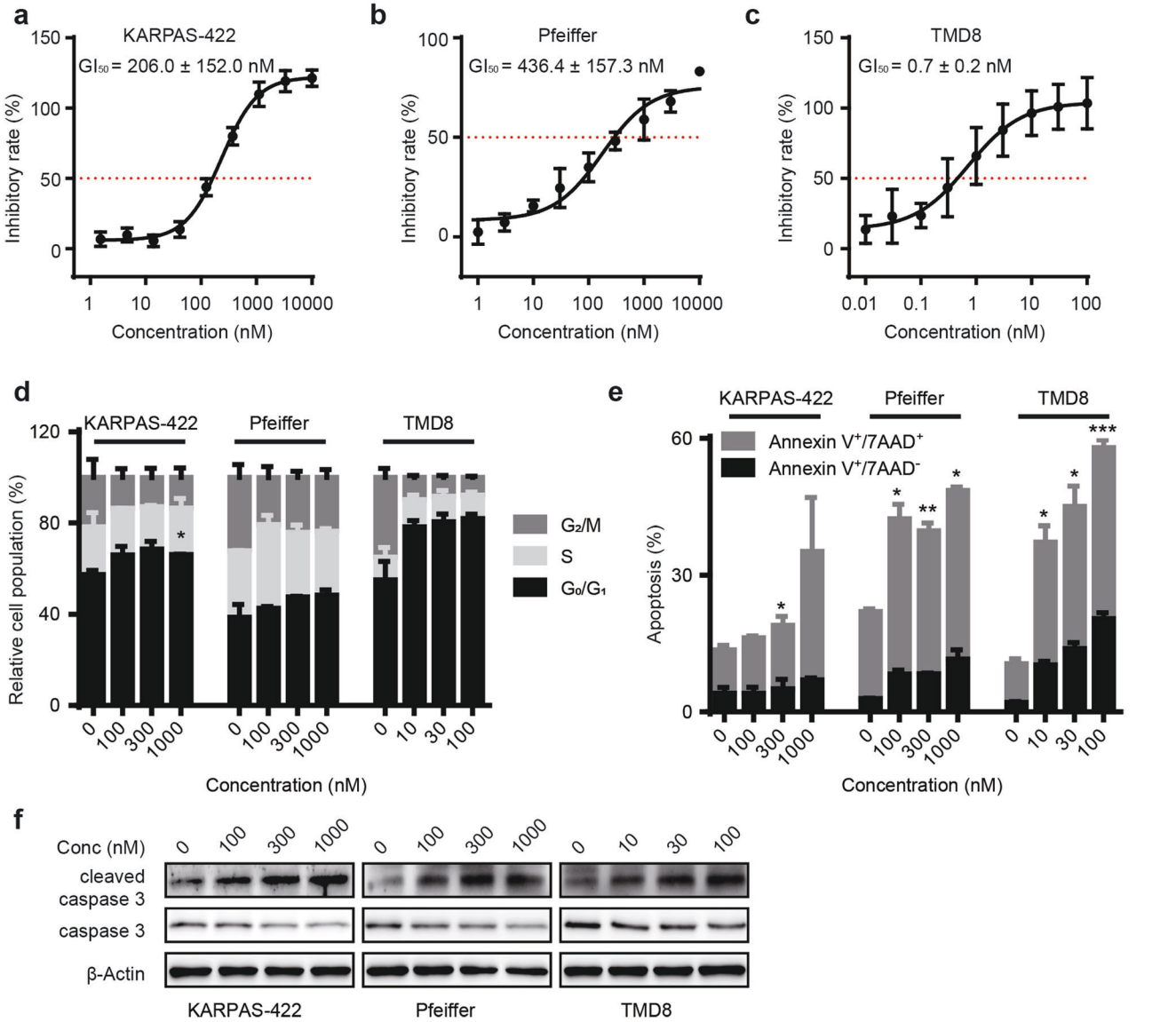

Fig. 4 SAF-248 induces cell cycle arrest and apoptosis in DLBCL cells. Growth inhibitory curves of SAF-248 in **a** KARPAS-422, **b** Pfeiffer, and **c** TMD8 cells. The tested cells were treated with SAF-248 for 72 h, and cell viability was determined by CCK-8 assay. **d** Induction of G_1 phase arrest by SAF-248 at the indicated concentrations for 24 h. Cell cycle analysis was performed by flow cytometry. **e**, **f** Induction of apoptosis by SAF-248 at the indicated concentrations for 72 h. **e** Apoptosis was detected by annexin V/7-AAD double staining. The data shown are the mean ± SD from two independent experiments. Statistical differences compared to vehicle control were analyzed with Student's *t* test. $^{*}P < 0.05$; $^{**}P < 0.01$; $^{***}P < 0.001$. **f** Cleavage of caspase 3 was detected by Western blot in KARPAS-422, Pfeiffer and TMD8 cells treated with SAF-248 at the indicated concentrations for 72 h.

60 mg/kg, respectively (Fig. 5a). Consistent with the results of the cell proliferation assay, SAF-248 displayed superior activity to idelalisib in inhibiting the growth of Pfeiffer xenografts. Although SAF-248 displayed similar efficacy at doses of 30 and 60 mg/kg in Pfeiffer xenografts, SAF-248 was able to inhibit the growth of TMD8 xenografts in a dose-dependent manner (Fig. 5c). SAF-248 at 100 mg/kg significantly inhibited TMD8 tumor growth with a *T*/C value of 12.5%. The diverse patterns of SAF-248 activity in different DLBCL xenografts may reflect the variable dependency of DLBCL on PI3Kδ. Moreover, SAF-248 did not cause significant weight loss in mice during the treatment (Fig. 5b, d), suggesting a favorable safety profile of SAF-248. To investigate whether SAF-248 inhibits PI3K signaling in tumor tissues, a single dose of SAF-248 at 100 mg/kg was orally administered to mice bearing TMD8 xenografts. Blood and tumors were collected at 2 and 4 h post treatment. As shown in Fig. 5e, SAF-248 showed concentrations of 4.9 μM and 2.5 μM in plasma and tumor tissues, respectively, at 2 h after administration and then decreased to 1.6 μM (plasma) and 0.7 μM (tumor tissues) 2 h later. Furthermore, the in vivo antitumor activity was well correlated with the inhibition of PI3K signaling, as indicated by the significant inhibition of AKT phosphorylation in tumor samples at 2 h after administration (Fig. 5f).

Prolonged treatment with SAF-248 activates the IL2/STAT5 signaling pathway

To investigate the effects of SAF-248 on the gene expression profile of TMD8 tumors, tumor tissues from TMD8 xenografts treated with 100 mg/kg SAF-248 for 8 h or 21 days were collected for RNAseq analysis. GSEA of differentially expressed genes was performed. As shown in Fig. 6a, gene sets of hallmarks for "IL2_STAT5", "IL6_STAT3", "MTORC1", and "MYC" were among the top enriched sets and were downregulated after treatment with

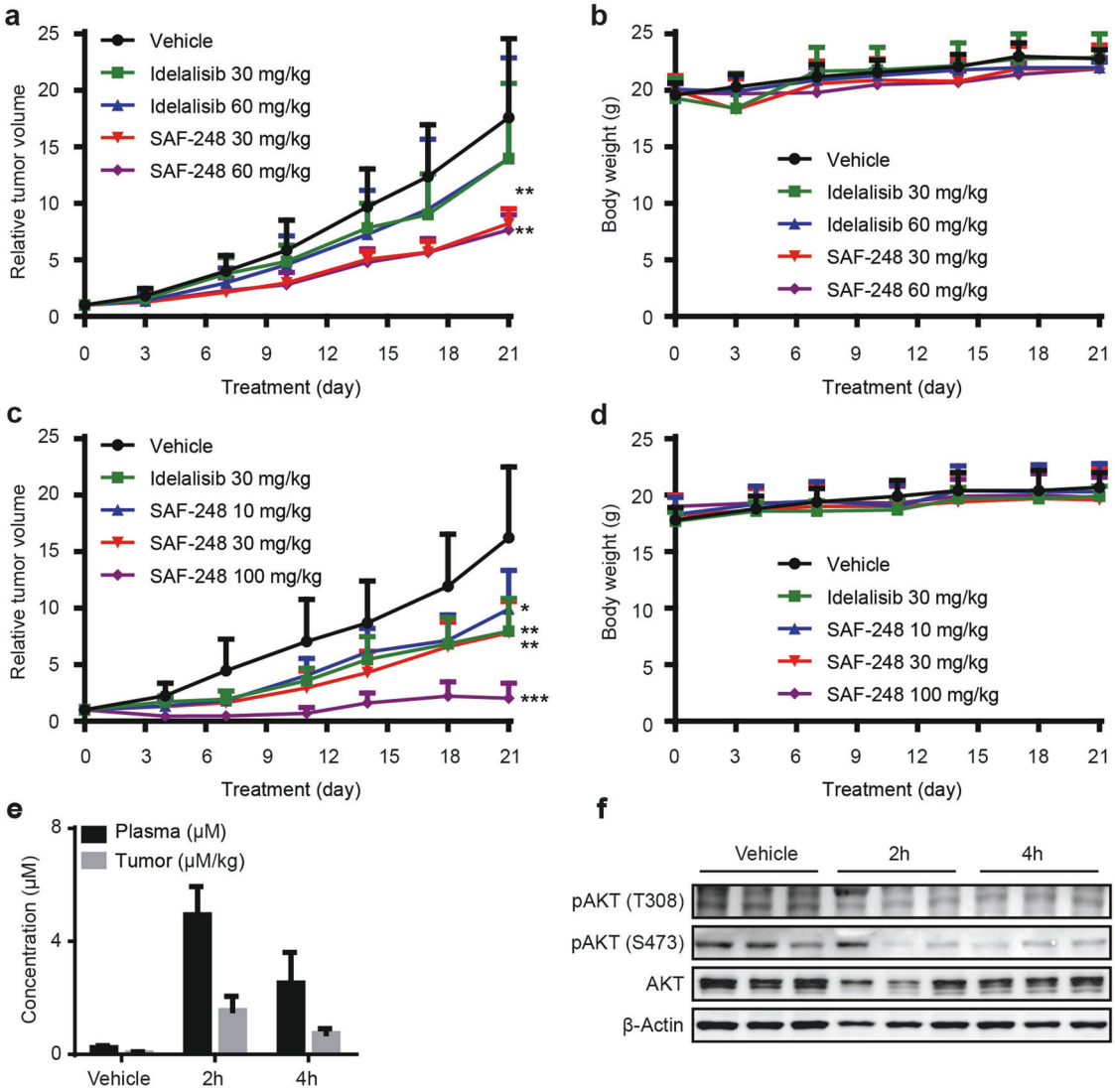

Fig. 5 SAF-248 suppresses tumor growth in Pfeiffer and TMD8 xenograft models. Antitumor efficacy and tumor weight after SAF-248 treatment in Pfeiffer (**a**, **b**) and TMD8 (**c**, **d**) xenografts. Tumor-bearing mice were orally administered vehicle control, idelalisib or SAF-248 at the indicated doses twice a day for 21 days. Tumor volumes were measured twice a week, and *T/C* values were calculated. Data presented are the mean ± SD of six mice in each group. Statistical differences compared to the vehicle group were analyzed with Student's *t* test. $^{*}P < 0.05$; $^{**}P < 0.01$; $^{***}P < 0.001$. **e**, **f** Mice bearing TMD8 tumors that received a single dose of SAF-248 at 100 mg/kg were sacrificed at the indicated times. **e** The concentration of SAF-248 in blood plasma and tumor tissues was determined. **f** Tumor tissues were collected, and lysates were analyzed by Western blot to detect the indicated proteins.

SAF-248 for 8 h. However, activation of "IL2_STAT5" and "IL6_STAT3" was observed after long-term (21 days) treatment. Furthermore, the gene signatures of multiple oncogenic pathways, such as "IL2_STAT5", "IL6_STAT3", "MTORC1" and "MYC", were upregulated in tumor tissues upon prolonged treatment with SAF-248 compared to those with short-term administration (Fig. 6b), suggesting that these signaling pathways might mediate cell survival upon continuous exposure to SAF-248.

The PI3K/AKT/mTOR signaling network is complex and involved in numerous feedback loops and crosstalk nodes with other signaling pathways. To confirm the results from TMD8 xenografts, the effects of SAF-248 on PI3K, STAT5, and STAT3 signaling were determined in TMD8 cells. As shown in Fig. 6c, the PI3K/mTOR signaling cascades responded quickly to SAF-248, as evidenced by decreases in phosphorylated AKT at T308 and S473, p70S6K (T389), pS6 (S240/244 and S35/236), and p4E-BP1 (T37/46) within 1 h of treatment, demonstrating a major role of PI3Kδ in constitutive PI3K signaling. Interestingly, phosphorylated AKT and S6 were gradually restored after exposure to SAF-248 for 24 h, whereas the phosphorylation of p70S6K and 4E-BP1 was persistently inhibited up to 72 h. SAF-248 at 10 nM significantly blocked Erk1/2 phosphorylation within 0.5 h and then restored 6 h after the treatment. Aberrant expression of STAT3 and STAT5 is found in DLBCL and may contribute to drug resistance in hematopoietic malignancies [31, 32]. Phosphorylation of STAT3 was blocked 3 h after SAF-248 treatment and then restored after longer treatment. A similar observation was obtained with STAT5. These results suggested that prolonged treatment with SAF-248 led to activation of both STAT5 and STAT3. Similarly, restoration of the MYC protein was observed 24 h after SAF-248 treatment despite decreased levels at earlier time points. These results were consistent with the gene expression data in TMD8 tumor xenografts (Fig. 6a), suggesting that these pathways may circumvent the activity of SAF-248.

To discover potential drug combinations that would enhance the activity of SAF-248, we screened the combinations of SAF-248

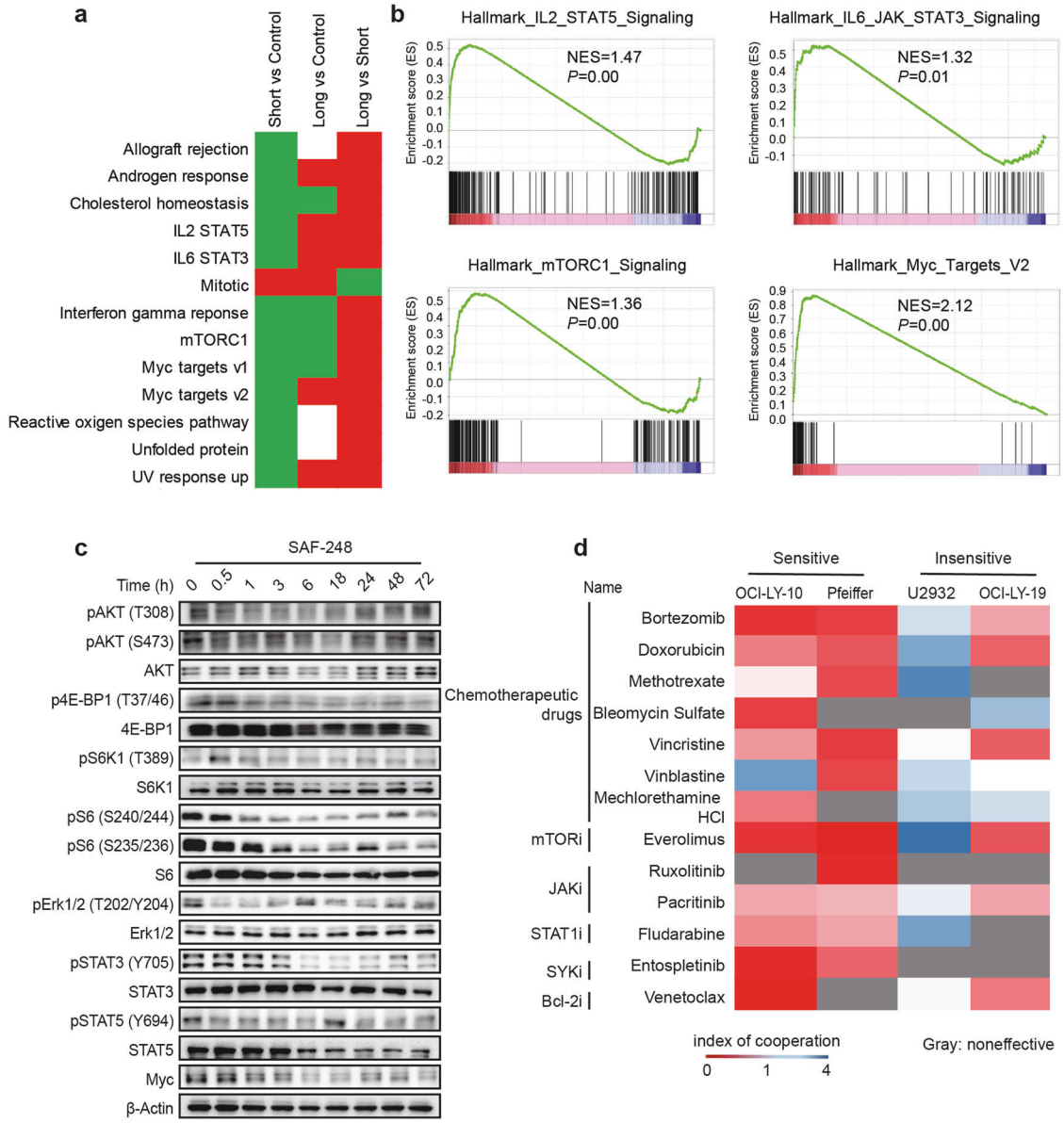

Fig. 6 Prolonged treatment with SAF-248 activates the IL2/STAT5 signaling pathway. a Heatmap of gene sets enriched by GSEA of the indicated groups. Tumors from the TMD8 xenografts treated with 100 mg/kg SAF-248 for 21 days or 8 h were collected for RNAseq analysis. mRNA expression data were further subjected to GSEA. Red indicates positively enriched gene sets, green denotes negatively enriched gene sets, and white represents no enrichment. **b** GSEA enrichment plot of differentially expressed genes between short- and long-term treatment with SAF-248. **c** TMD8 cells treated with SAF-248 (10 nM) and collected at the indicated times for Western blot analysis. **d** The combinatorial effect of SAF-248 and the indicated compound against the proliferation of the indicated DLBCL cell lines. Tested cells were seeded in 96-well plates and incubated with different concentrations of each compound or the indicated combination for 72 h in triplicate. Cell proliferation was detected by CCK-8 assay. Synergistic effects were analyzed using CalcuSyn software.

with approved drugs or candidates in clinical trials for the treatment of DLBCL in four DLBCL cell lines. The combinatorial effects were evaluated by calculating the CI using CalcuSyn software, where $CI < 1$ denotes synergy, $CI = 1$ indicates an additive effect and $CI > 1$ reflects antagonism. As shown in Fig. 6d, SAF-248 showed synergistic effects in inhibiting the proliferation of sensitive OCI-LY-10 (ABC-DLBCL) and Pfeiffer (GCB-DLBCL) cells when combined with most of the tested drugs. No synergy was observed in insensitive U2932 (ABC-DLBCL) cells, whereas 7 out of 13 compounds exhibited synergistic effects with SAF-248 in insensitive OCY-LY-19 (GCB-DLBCL) cells. Synergism was observed in 3 of 4 evaluated DLBCL cell lines when SAF-248 was combined with pacritinib, a JAK2/FLT3 inhibitor. A similar effect was also observed for the combination of SAF-248 with the mTOR inhibitor everolimus.

DISCUSSION

The PI3Kδ pathway is one of the most dysregulated signaling pathways in B-cell hematologic malignancies and has become an attractive therapeutic target [33]. In this study, we reported that a novel PI3Kδ-selective inhibitor, SAF-248, possessed potent activity against DLBCL in vitro and in vivo. SAF-248 exhibited a 6- to 34-fold greater inhibitory effect on PI3Kδ than on other PI3K isoforms. SAF-248 induced G_1 phase cell cycle arrest and apoptosis in DLBCL cells. Profiling of the activity of SAF-248 in a panel of DLBCL cell

lines revealed that PI3Kα expression was negatively correlated with the antiproliferative activity of SAF-248. Moreover, compensatory overactivation of the PI3K/AKT/mTOR, JAK/STAT and MYC signaling pathways might circumvent the activity of SAF-248, which could be overcome by concurrent inhibition of PI3Kδ and the corresponding signaling pathway.

SAF-248 presented similar yet superior activity against a panel of lymphoma cells compared to idelalisib, the first oral PI3Kδ inhibitor approved for the treatment of relapsed CLL, SLL, and FL. Although idelalisib shows significant efficacy, it also presents serious toxicity. Shin et al. proposed that hepatotoxicity associated with PI3Kδ inhibitors was structure-based rather than mechanism-based [34]. Compared to idelalisib, SAF-248 possesses a novel structure, which may lead to a different reaction pattern with p110δ. Notably, our study demonstrated that SAF-248 achieved concentrations sufficient to inhibit tumor growth without showing substantial toxicity, indicating that it was well tolerated. A better understanding of the binding mode of SAF-248 with PI3Kδ may provide a strategy for the design of new, more potent inhibitors against PI3Kδ.

Although PI3Kδ has been recognized as the dominant isoform in B-cell malignancies, we failed to identify a significant correlation between the expression of PI3Kδ and the activity of SAF-248 in the tested DLBCL cells. In contrast, we found that the expression of PI3Kα was negatively correlated with the activity of SAF-248, indicating an important role of PI3Kα in the proliferation of DLBCL cells. Overexpression of PI3Kα is frequently found in DLBCL and is correlated with poor prognosis [35], which has been proposed as a potential mechanism for the intrinsic resistance of DLBCL to PI3Kδ inhibition in clinical settings [36]. Similarly, Joel et al. reported that a high PIK3CA/PIK3CD mRNA ratio could predict resistance to PI3Kδ-selective inhibition in mantle cell lymphoma [37]. A high level of phosphorylated AKT is often found in DLBCL and has been considered a prognostic factor. However, AKT phosphorylation did not exhibit a correlation with the activity of SAF-248 in the panel of tested DLBCL cell lines. Due to the small number of cell lines tested in this study, further investigation with an increased sample size as well as examination in the clinical setting is required.

Although PI3Kδ inhibitors have exhibited promising clinical efficacy, patients may develop adaptive resistance after an initial favorable response. By profiling the gene expression in TMD8 xenografts, we found that multiple oncogenic pathways, such as IL2_STAT5, IL6_STAT3, MTORC1 and MYC, were upregulated in tumor tissues upon prolonged treatment with SAF-248 compared to those with short-term administration, which was further confirmed in cultured TMD8 cells. These results indicated that the reactivation of the aforementioned signaling pathways may circumvent the efficacy of PI3Kδ inhibitors. MYC is one of the most common oncogenes in DLBCL, and knockdown of MYC reverses resistance to PI3K inhibitors [38, 39]. Similarly, the IL6-JAK-STAT cascade was found to play a critical role leading to the resistance of lymphoma cells to copanlisib and duvelisib [40]. Consistent with these observations, simultaneous targeting of PI3Kδ and mTOR, MYC or JAK-STAT synergistically inhibited the proliferation of SAF-248-sensitive DLBCL cells. Notably, few of the tested compounds displayed synergy with SAF-248 in resistant DLBCL U2932 and OCY-LY-19 cells, suggesting that the intrinsic resistance to PI3Kδ might not be able to be overcome by a drug combination. Although this finding needs to be further validated in vivo and in clinical trials, it provides new clues to enhance the efficacy of PI3Kδ inhibitors via rational drug combinations.

In summary, SAF-248 is a novel and highly potent PI3Kδ-selective inhibitor with promising activity against DLBCL in vitro and in vivo, making it a promising candidate for the treatment of DLBCL. The potential mechanisms of resistance and drug combinations may provide useful insights for the clinical development of PI3Kδ inhibitors for the treatment of DLBCL.

ACKNOWLEDGEMENTS

This work was supported by the "Personalized Medicines-Molecular Signature-based Drug Discovery and Development", Strategic Priority Research Program of the Chinese Academy of Sciences (XDA12020235) and the National Science and Technology Major Project "Key New Drug Creation and Manufacturing Program" (2018ZX09711002-004-004). We thank Shu Lin and Jia-shu Zhou (Department of Biology, Fochon Pharmaceuticals, Ltd.) for proofreading the manuscript.

AUTHOR CONTRIBUTIONS

XZ and LHM designed the research; XZ, YTD, and YW performed the experiments and analyzed the data; XDZ and ZWZ designed and synthesized the compound; YMS, DZL, and YC performed the in vivo experiments. YXW performed CI analysis. YXL and LHJ contributed to early screening and identification of the compound; XZ performed the bioinformatics analysis; XZ and LHM drafted the manuscript; and MYG, JD, and LHM supervised the study.

ADDITIONAL INFORMATION

Competing interests: Xing-dong Zhao, Zu-wen Zhou,Yan-xin Liu and Li-hua Jiang are employees of Fochon Pharmaceuticals, Ltd..

REFERENCES

1. Miao Y, Medeiros LJ, Li Y, Li J, Young KH. Genetic alterations and their clinical implications in DLBCL. Nat Rev Clin Oncol. 2019;16:634–52.
2. Roschewski M, Staudt LM, Wilson WH. Diffuse large B-cell lymphoma-treatment approaches in the molecular era. Nat Rev Clin Oncol. 2014;11:12–23.
3. Coiffier B, Sarkozy C. Diffuse large B-cell lymphoma: R-CHOP failure-what to do? Hematol Am Soc Hematol Educ Program. 2016;2016:366–78.
4. Bojarczuk K, Bobrowicz M, Dwojak M, Miazek N, Zapala P, Bunes A, et al. B-cell receptor signaling in the pathogenesis of lymphoid malignancies. Blood Cells Mol Dis. 2015;55:255–65.
5. Fruman DA, Chiu H, Hopkins BD, Bagrodia S, Cantley LC, Abraham RT. The PI3K pathway in human disease. Cell. 2017;170:605–35.
6. Hawkins PT, Anderson KE, Davidson K, Stephens LR. Signalling through Class I PI3Ks in mammalian cells. Biochem Soc Trans. 2006;34:647–62.
7. Okkenhaug K, Vanhaesebroeck B. PI3K in lymphocyte development, differentiation and activation. Nat Rev Immunol. 2003;3:317–30.
8. Okkenhaug K, Bilancio A, Emery JL, Vanhaesebroeck B. Phosphoinositide 3-kinase in T cell activation and survival. Biochem Soc Trans. 2004;32:332–5.
9. Lampson BL, Brown JR. PI3Kdelta-selective and PI3Kalpha/delta-combinatorial inhibitors in clinical development for B-cell non-Hodgkin lymphoma. Expert Opin Investig Drugs. 2017;26:1267–79.
10. Flinn IW, O'Brien S, Kahl B, Patel M, Oki Y, Foss FF, et al. Duvelisib, a novel oral dual inhibitor of PI3K-delta,gamma, is clinically active in advanced hematologic malignancies. Blood. 2018;131:877–87.
11. Dreyling M, Santoro A, Mollica L, Leppa S, Follows GA, Lenz G, et al. Phosphatidylinositol 3-kinase inhibition by copanlisib in relapsed or refractory indolent lymphoma. J Clin Oncol. 2017;35:3898–905.
12. Oki Y, Kelly KR, Flinn I, Patel MR, Gharavi R, Ma A, et al. CUDC-907 in relapsed/refractory diffuse large B-cell lymphoma, including patients with MYC-alterations: results from an expanded phase I trial. Haematologica. 2017;102:1923–30.
13. Miao Y, Medeiros LJ, Xu-Monette ZY, Li J, Young KH. Dysregulation of cell survival in diffuse large B cell lymphoma: mechanisms and therapeutic targets. Front Oncol. 2019;9:107.
14. Greenwell IB, Ip A, Cohen JB. PI3K inhibitors: understanding toxicity mechanisms and management. Oncology. 2017;31:821–8.
15. Fruman DA, Rommel C. PI3K and cancer: lessons, challenges and opportunities. Nat Rev Drug Discov. 2014;13:140–56.
16. Klempner SJ, Myers AP, Cantley LC. What a tangled web we weave: emerging resistance mechanisms to inhibition of the phosphoinositide 3-kinase pathway. Cancer Discov. 2013;3:1345–54.
17. Zhao XD, Ding J, Meng LH, Geng MY, Li TS, Zhou ZW, et al. inventors; Shanghai Fochon Pharmaceutical Co., Ltd., Shanghai Institute of Materia Medica Chinese Academy of Sciences, Chongqing Fochon Pharmaceutical Co., Ltd., assignees. Certain protein kinase inhibitors. US patent 10328060 B2. 2019 June 25.
18. Yang X, Zhang X, Huang M, Song K, Li X, Huang M, et al. New insights into PI3K inhibitor design using X-ray structures of PI3Kalpha complexed with a potent lead compound. Sci Rep. 2017;7:14572.

19. Yang C, Zhang X, Wang Y, Yang Y, Liu X, Deng M, et al. Discovery of a novel series of 7-azaindole scaffold derivatives as PI3K inhibitors with potent activity. ACS Med Chem Lett. 2017;8:875–80.
20. Wang X, Zhang X, Li BS, Zhai X, Yang Z, Ding LX, et al. Simultaneous targeting of PI3Kdelta and a PI3Kdelta-dependent MEK1/2-Erk1/2 pathway for therapy in pediatric B-cell acute lymphoblastic leukemia. Oncotarget. 2014;5:10732–44.
21. Xiang HY, Wang X, Chen YH, Zhang X, Tan C, Wang Y, et al. Identification of methyl (5-(6-((4-(methylsulfonyl)piperazin-1-yl)methyl)-4-morpholinopyrrolo[2,1-f][1,2,4]triazin-2-yl)-4-(trifluoromethyl)pyridin-2-yl)carbamate (CYH33) as an orally bioavailable, highly potent, PI3K alpha inhibitor for the treatment of advanced solid tumors. Eur J Med Chem. 2021;209:112913.
22. Shi JJ, Xing H, Wang YX, Zhang X, Zhan QM, Geng MY, et al. PI3Kalpha inhibitors sensitize esophageal squamous cell carcinoma to radiation by abrogating survival signals in tumor cells and tumor microenvironment. Cancer Lett. 2019; 459:145–55.
23. Wei M, Zhang X, Wang X, Song Z, Ding J, Meng LH, et al. SAR study of 5-alkynyl substituted quinazolin-4(3H)-ones as phosphoinositide 3-kinase delta (PI3Kdelta) inhibitors. Eur J Med Chem. 2017;125:1156–71.
24. Elkabets M, Vora S, Juric D, Morse N, Mino-Kenudson M, Muranen T, et al. mTORC1 inhibition is required for sensitivity to PI3K p110alpha inhibitors in PIK3CA-mutant breast cancer. Sci Transl Med. 2013;5:196ra199.
25. Shin N, Li YL, Mei S, Wang KH, Hall L, Katiyar K, et al. INCB040093 Is a novel PI3Kdelta inhibitor for the treatment of B cell lymphoid malignancies. J Pharmacol Exp Ther. 2018;364:120–30.
26. Xie C, He Y, Zhen M, Wang Y, Xu Y, Lou L. Puquitinib, a novel orally available PI3Kdelta inhibitor, exhibits potent antitumor efficacy against acute myeloid leukemia. Cancer Sci. 2017;108:1476–84.
27. Havranek O, Xu J, Kohrer S, Wang Z, Becker L, Comer JM, et al. Tonic B-cell receptor signaling in diffuse large B-cell lymphoma. Blood. 2017;130:995–1006.
28. Pfeifer M, Grau M, Lenze D, Wenzel SS, Wolf A, Wollert-Wulf B, et al. PTEN loss defines a PI3K/AKT pathway-dependent germinal center subtype of diffuse large B-cell lymphoma. Proc Natl Acad Sci USA. 2013;110:12420–5.
29. Erdmann T, Klener P, Lynch JT, Grau M, Vockova P, Molinsky J, et al. Sensitivity to PI3K and AKT inhibitors is mediated by divergent molecular mechanisms in subtypes of DLBCL. Blood. 2017;130:310–22.
30. Young RM, Wu T, Schmitz R, Dawood M, Xiao W, Phelan JD, et al. Survival of human lymphoma cells requires B-cell receptor engagement by self-antigens. Proc Natl Acad Sci USA. 2015;112:13447–54.
31. Dorritie KA, McCubrey JA, Johnson DE. STAT transcription factors in hematopoiesis and leukemogenesis: opportunities for therapeutic intervention. Leukemia. 2014;28:248–57.
32. Brachet-Botineau M, Polomski M, Neubauer HA, Juen L, Hedou D, Viaud-Massuard MC, et al. Pharmacological inhibition of oncogenic STAT3 and STAT5 signaling in hematopoietic cancers. Cancers. 2020;12:240–87.
33. Preite S, Gomez-Rodriguez J, Cannons JL, Schwartzberg PL. T and B-cell signaling in activated PI3K delta syndrome: from immunodeficiency to autoimmunity. Immunol Rev. 2019;291:154–73.
34. Shin N, Stubbs M, Koblish H, Yue EW, Soloviev M, Douty B, et al. Parsaclisib Is a next-generation phosphoinositide 3-kinase delta inhibitor with reduced hepatotoxicity and potent antitumor and immunomodulatory activities in models of B-cell malignancy. J Pharmacol Exp Ther. 2020;374:211–22.
35. Paul J, Soujon M, Wengner AM, Zitzmann-Kolbe S, Sturz A, Haike K, et al. Simultaneous inhibition of PI3Kdelta and PI3Kalpha Induces ABC-DLBCL regression by blocking BCR-dependent and -independent activation of NF-kappaB and AKT. Cancer Cell. 2017;31:64–78.
36. Pongas GN, Annunziata CM, Staudt LM. PI3Kdelta inhibition causes feedback activation of PI3Kalpha in the ABC subtype of diffuse large B-cell lymphoma. Oncotarget. 2017;8:81794–802.
37. Iyengar S, Clear A, Bodor C, Maharaj L, Lee A, Calaminici M, et al. P110alpha-mediated constitutive PI3K signaling limits the efficacy of p110delta-selective inhibition in mantle cell lymphoma, particularly with multiple relapse. Blood. 2013;121:2274–84.
38. Xia B, Tian C, Guo S, Zhang L, Zhao D, Qu F, et al. c-Myc plays part in drug resistance mediated by bone marrow stromal cells in acute myeloid leukemia. Leuk Res. 2015;39:92–9.
39. Dey N, Leyland-Jones B, De P. MYC-xing it up with PIK3CA mutation and resistance to PI3K inhibitors: summit of two giants in breast cancers. Am J Cancer Res. 2015;5:1–19.
40. Kim JH, Kim WS, Park C. Interleukin-6 mediates resistance to PI3K-pathway-targeted therapy in lymphoma. BMC Cancer. 2019;19:936.